Exploration of Binary Virus–Host Interactions Using an Infectious Protein Complementation Assay*[S]

Sandie Munier‡§¶, Thomas Rolland‖, Cédric Diot‡§¶, Yves Jacob‡§¶‖**‡‡, and Nadia Naffakh‡§¶‡‡**

A precise mapping of pathogen–host interactions is essential for comprehensive understanding of the processes of infection and pathogenesis. The most frequently used techniques for interactomics are the yeast two-hybrid binary methodologies, which do not recapitulate the pathogen life cycle, and the tandem affinity purification mass spectrometry co-complex methodologies, which cannot distinguish direct from indirect interactions. New technologies are thus needed to improve the mapping of pathogen–host interactions. In the current study, we detected binary interactions between influenza A virus polymerase and host proteins during the course of an actual viral infection, using a new strategy based on trans-complementation of the Gluc1 and Gluc2 fragments of *Gaussia princeps* luciferase. Infectious recombinant influenza viruses that encode a Gluc1-tagged polymerase subunit were engineered to infect cultured cells transiently expressing a selected set of Gluc2-tagged cellular proteins involved in nucleocytoplasmic trafficking pathways. A random set and a literature-curated set of Gluc2-tagged cellular proteins were tested in parallel. Our assay allowed the sensitive and accurate recovery of previously described interactions, and it revealed 30% of positive, novel viral–host protein–protein interactions within the exploratory set. In addition to cellular proteins involved in the nuclear import pathway, components of the nuclear pore complex such as NUP62 and mRNA export factors such as NXF1, RMB15B, and DDX19B were identified for the first time as interactors of the viral polymerase. Gene silencing experiments further showed that NUP62 is required for efficient viral replication. Our findings give new insights regarding the subversion of host nucleocytoplasmic trafficking pathways by influenza A viruses. They also demonstrate the potential of our infectious protein complementation assay for high-throughput exploration of influenza virus interactomics in infected cells. With more infectious reverse genetics systems becoming available, this strategy should be widely applicable to numerous pathogens. ***Molecular & Cellular Proteomics 12: 10.1074/mcp.M113.028688, 2845–2855, 2013.***

Influenza pandemics can be devastating. Even during typical epidemic years, ~250,000 to 500,000 people worldwide die as a result of severe complications associated with influenza infections. The elucidation of how influenza viruses interact with the host cell machinery and hijack cellular pathways has become an active field of research and could pave the way to new antiviral approaches targeting virus–host interactions (1, 2). Several RNAi-based genome-wide screens have been performed for the identification of host factors involved in influenza virus replication (3–9). Because influenza virus polymerase is a key component in the viral life cycle and is a strong determinant of virulence and host range (10, 11), other studies have used yeast two-hybrid (9, 12) or proteomics approaches (13–15) to attempt to identify cellular proteins that interact with the viral polymerase. These approaches have limitations, as they do not recapitulate the entire viral cycle or cannot distinguish between direct and indirect interactions (16). New technologies are thus needed to improve the mapping of virus–host interactions and to aid in the design of more effective therapeutics.

The genome of influenza A viruses consists of eight molecules of single-stranded RNA of negative polarity. The viral RNAs associate with the nucleoprotein and with the three subunits of the polymerase complex (PB1, PB2, and PA) to form ribonucleoproteins (RNPs).[1] Once in the infected cells, the RNPs are transported to the nucleus, where they undergo transcription and replication (17). We used a new strategy to

From the ‡Institut Pasteur, Unité de Génétique Moléculaire des Virus à ARN, Département de Virologie, F-75015 Paris, France; §CNRS, UMR3569, F-75015 Paris, France; ¶Université Paris Diderot, Sorbonne Paris Cité, Unité de Génétique Moléculaire des Virus à ARN, EA302, F-75015 Paris, France; ‖Center for Cancer Systems Biology (CCSB) and Department of Cancer Biology, Dana-Farber Cancer Institute, Boston, Massachusetts 02215; **Department of Genetics, Harvard Medical School, Boston, Massachusetts 02115

Received February 22, 2013, and in revised form, June 6, 2013
Published, MCP Papers in Press, July 1, 2013, DOI 10.1074/mcp.M113.028688

[1] The abbreviations used are: GO, gene ontology; iPCA, infectious protein complementation assay; LCS, literature-curated set; MOI, multiplicity of infection; MS, mass spectrometry; NLR, normalized luminescence ratio; NPC, nuclear pore complex; pfu, particle forming unit; PPI, protein–protein interaction; RNP, ribonucleoproteins; RRS, random reference set; TPCK, L-1-tosylamido-2-phenylethyl chloromethyl ketone; VSV, vesicular stomatitis virus.

detect binary interactions between the viral polymerase and host proteins during the course of an actual viral infection. Our infectious protein complementation assay (iPCA) is based on the complementation of two trans-complementing fragments of *Gaussia princeps* luciferase, Gluc1 and Gluc2 (18, 19). Interaction-mediated luciferase activity is measured in cultured cells transiently expressing a cellular protein fused to Gluc2 and infected with a recombinant influenza virus having Gluc1 fused to one of its polymerase subunits. These engineered infectious viruses allowed us to achieve the sensitive and accurate detection of influenza virus–host protein–protein interactions throughout the viral cycle.

EXPERIMENTAL PROCEDURES

Cells and Viruses—293T, A549, and BSR cells were grown in complete Dulbecco's modified Eagle's medium (DMEM) supplemented with 10% fetal calf serum (FCS). MDCK cells were grown in modified Eagle's medium supplemented with 5% FCS.

Wild-type A/WSN/33 (WSN) influenza virus was produced via reverse genetics using a procedure adapted from the work of Fodor *et al.* (20). Vesicular stomatitis virus (VSV) (Indiana strain) was kindly provided by O. Delmas (Institut Pasteur, Paris, France). WSN and VSV viruses were amplified on MDCK and BSR cells, respectively, at a multiplicity of infection (MOI) of 0.001 pfu/cell. They were titrated on MDCK and BSR cells, respectively, using a plaque assay adapted from Matrosovich *et al.* (21).

Plasmids—The eight pPolI plasmids containing the sequences corresponding to the genomic segments of influenza virus A/WSN/33 and the four recombinant pcDNA3.1 plasmids for the expression of WSN-PB1, -PB2, -PA, and -NP proteins (20) were kindly provided by G. Brownlee (Sir William Dunn School of Pathology, Oxford, UK).

The pPolI-SL-PB2-Gluc1 and pPolI-SL-PB2-Gluc2 plasmids were obtained by subcloning the Gluc1 and Gluc2 coding sequences, respectively, between the NotI and NheI sites of the pPolI-PB2-GFPS11 plasmid (22).

The pPolI-PB1-SL-Gluc1 and pPolI-PA-LL-Gluc1 plasmids were obtained via modification of the pPolI-WSN-PB1 and pPolI-WSN-PA using standard PCR and cloning procedures in order to fuse the following sequences to the 5′ end of the PB1- or PA-ORF: (a) a short sequence encoding the short peptidic linker AAAGGS (SL, for PB1) or the long peptidic linker AAAGGGGSGGGGS (LL, for PA); (b) the Gluc1 coding sequence; (c) a stop codon combined with an SpeI restriction site (TAAACTAGT); and (d) the 5′ terminal 88 nucleotides of the PB1 segment or the 5′ terminal 100 nucleotides of the PA segment.

To produce the pPolI-PB1-SL-Gluc2 and pPolI-PA-LL-Gluc2 plasmids, the Gluc2 coding sequence was amplified using the pSPICA-N2 plasmid (18) as a template. The resulting PCR product was digested with NotI and NheI and subcloned between the NotI and SpeI sites of pPolI-PB1-Gluc1 and pPolI-PA-Gluc1 plasmids, respectively.

The Gateway®-compatible donor plasmids containing cellular Open Reading Frames (ORFs) were obtained from the Human ORFeome resource (hORFeome v3.1). They were transferred into the Gateway®-compatible pSPICA-N2 destination vector (18) using LR clonase (Invitrogen) according to the manufacturer's specifications. The resulting plasmids allowed the expression of Gluc2-cellular-ORF fusion proteins.

The proteins included in the random reference set (RRS) were randomly selected from within the RRS used by Braun *et al.* (23).

All constructs were verified through sequencing using a Big Dye terminator sequencing kit and an automated sequencer (PerkinElmer Life Sciences). The sequences of the oligonucleotides used for amplification and sequencing can be provided upon request.

Production of Recombinant Viruses via Reverse Genetics—The method used for the production of recombinant influenza viruses via reverse genetics was adapted from previously described procedures (20). Briefly, the eight pPolI-WSN and four pcDNA3.1-WSN plasmids (0.5 μg of each) were co-transfected into a sub-confluent monolayer of co-cultivated 293T and MDCK cells (4×10^5 and 3×10^5 cells, respectively, seeded in a 35-mm dish) using 10 μl of FuGENE® HD transfection reagent (Roche). After 24 h of incubation at 35 °C, the supernatant was removed, and cells were washed twice with DMEM and incubated at 35 °C in DMEM containing TPCK-treated trypsin at a final concentration of 1 μg/ml for 48 h. The efficiency of reverse genetics was evaluated by titrating the supernatant on MDCK cells in plaque assays. For subsequent amplification of the recombinant PB1-, PB2-, and PA-Gluc1 or PB1-, PB2-, and PA-Gluc2 viruses, MDCK cells were infected at an MOI of 0.0001 and incubated for 3 days at 35 °C in DMEM containing TPCK-treated trypsin at a concentration of 1 μg/ml. Viral stocks were titrated via plaque assays on MDCK cells as described elsewhere (21). Viral RNA was extracted and subjected to reverse-transcription and amplification using specific oligonucleotides. The products of amplification were purified using a QIAquick gel extraction kit (Qiagen, Courtaboeuf, France) and were sequenced using a Big Dye terminator sequencing kit and an automated sequencer (PerkinElmer Life Sciences). The sequences of the oligonucleotides used for amplification and sequencing can be provided upon request.

Antiviral Activity Assay—MDCK cells were seeded at a concentration of 2×10^4 cells per well in 96-well white plates (Greiner Bio-One, Courtaboeuf, France). After 24 h, cells were rinsed twice with DMEM and co-infected with a combination of vP-Gluc1 and vP′-Gluc2 viruses (0.01 pfu of each virus/cell in 50 μl). After viral adsorption for 1 h at 35 °C, 50 μl of DMEM supplemented with 4% of FCS were added and cells were incubated at 35 °C for 24 h. Cells were either left untreated or incubated with ribavirin (Sigma) or nucleozin (Sigma) at a final concentration of 1–100 μM or 0.01–1 μM, respectively, for 24 h post-infection, or they were incubated with amantadine (Sigma) at a final concentration of 10 μM during the 30 min preceding infection, during viral adsorption, and for 24 h post-infection. At 24 h post-infection, cells were mildly rinsed in Ca^{2+}/Mg^{2+}-Dulbecco's PBS, and 40 μl of *Renilla* lysis buffer (Promega, Charbonnières, France) were directly added to each well. After incubation for 1 h at room temperature, the *Gaussia princeps* luciferase enzymatic activity was measured using the *Renilla* luciferase assay reagent (Promega) and a Berthold Centro XS luminometer (*Renilla* luminescence counting program, integration time of 10 s after injection of 50 μl of the reagent).

Viral–Host Protein–Protein Interaction Assay—293T cells were seeded at a concentration of 3×10^4 cells per well in 96-well white plates (Greiner Bio-One, Courtaboeuf, France). After 24 h, the cells were co-transfected in triplicate with 100 ng of the recombinant p-Gluc2-cellular-ORF constructs and 50 ng of the pCI plasmid (Promega) using polyethyleneimine (Polysciences Inc, Le Perray-en-Yvelines, France). At 17 h post-transfection, cells were rinsed with DMEM and infected with 50 μl of a viral suspension containing 9×10^5 pfu of PB2-Gluc1, PB1-Gluc1, or PA-Gluc1 recombinant virus.

As a control, cells were either (i) co-transfected with 100 ng of the empty p-Gluc2 plasmid and 50 ng of pCI and subsequently infected with 9×10^5 pfu of PB2-Gluc1, PB1-Gluc1, or PA-Gluc1 recombinant virus or (ii) co-transfected with 100 ng of the p-Gluc2-cellular-ORF constructs and 50 ng of the empty p-Gluc1 plasmid and subsequently infected with 9×10^5 pfu of the wild-type WSN virus.

After viral adsorption for 1 h at 35 °C, 50 μl of DMEM supplemented with 4% FCS were added to each well, and cells were incubated at 35 °C for 6 h. Cells were mildly rinsed in Ca^{2+}/Mg^{2+}-Dulbecco's PBS, and 40 μl of *Renilla* lysis buffer (Promega) were

directly added to each well. After incubation for 1 h at room temperature, the *Gaussia princeps* luciferase enzymatic activity was measured using the *Renilla* luciferase assay reagent (Promega) and a Berthold Centro XS luminometer (*Renilla* luminescence counting program, integration time of 2 s after injection of 50 μl of the reagent). For each p-Gluc2-cellular-ORF plasmid, three normalized luminescence ratios (NLRs) were calculated as follows: the luminescence activity measured in cells transfected with the p-Gluc2-cellular-ORF plasmid and infected with the PB2-Gluc1, PB1-Gluc1, or PA-Gluc1 virus (arbitrary units, mean of triplicates) was divided by the sum of the luminescence activities measured in both control samples as described above (arbitrary units, mean of triplicates).

Enrichment Analysis—The integrated dataset of human protein–protein interactions (PPIs) available in the HIPPIE database was used to generate the subnetwork of PPIs connected as first neighbors to proteins directly targeted by the influenza virus polymerase subunits (layer one). This subset of PPIs connected to layer one was scored according to experimental evidence as described in HIPPIE (24). Interactions with scores greater than or equal to 0.75, considered as high-confidence interactions, were selected as layer two. The resulting subnetwork was analyzed with ClueGO (Cytoscape plugin (25)) to extract the non-redundant biological information based on enrichment for biological process descriptors in gene ontology (GO) annotations associated with each polymerase subunit. The significance of each term was calculated using a hypergeometric test and a Bonferroni *p* value correction according to ClueGO standard statistical options (25). GO term analysis was restricted to *p* values $\leq$ 0.01 and "global" network predefined selection criteria in order to get more global functional enrichment information and obtain insights into the main biological processes susceptible to targeting by the influenza virus polymerase subunits.

siRNA Transfection and Infection Assays—Small interfering RNAs (siRNAs) targeting CCT2, RANGAP1, and NUP62 were purchased from Thermo Scientific (Illkirch, France). Non-target siRNA (Dharmacon ON-TARGETplus Non-targeting Control pool) was used as a negative control. A549 cells (2×10^4 cells) were transfected in suspension with 25 nM of siRNA using 0.2 μl of DharmaFECT1 transfection reagent (Thermo Scientific) and were plated in 96-well plates. The medium was replaced with fresh medium 24 h later. At 48 h post-transfection, cells were infected with influenza A/WSN/33 virus at an MOI of 0.001 pfu/cell or with VSV at an MOI of 0.0001 pfu/cell. After viral adsorption for 1 h at 37 °C, 50 μl of DMEM supplemented with 4% FCS were added per well and cells were incubated at 37 °C for 24 h. Supernatants were collected and viral titers were determined via plaque assays on MDCK or BSR cells as described above. Cell viability was determined by assaying the total intracellular ATP with the CellTiter-Glo Luminescent Viability Assay kit (Promega) according to the manufacturer's recommendations. Down-regulation of siRNA-targeted genes was evaluated at 48 h and 72 h post-transfection by means of RT-qPCR using the Maxima First Strand cDNA Synthesis Kit and Solaris qPCR Expression Assays and Master Mix (Thermo Scientific) according to the manufacturer's recommendations.

RESULTS

Using a plasmid-based reverse genetics system (20, 26, 27), we produced a set of infectious recombinant A/WSN/33 (WSN) influenza viruses that expressed a PB1, PB2, or PA polymerase subunit fused at their C-terminal end to Gluc1 or Gluc2 complementation fragments of *Gaussia princeps* luciferase. Viability of the recombinant viruses depended on the peptidic linker separating the Gluc fragment from the polymerase subunits, and on sequence duplication ensuring the conservation of packaging signals at the 5′ end of the viral genomic segments (26) (Fig. 1). Despite moderate attenuation relative to the wild-type WSN virus, the viruses expressing a viral fusion protein (vP-Gluc1 or vP-Gluc2) were replication-competent, with the vP-Gluc1 viruses showing higher titers than their vP-Gluc2 counterparts upon multi-cycle amplification on MDCK cells (2×10^6 to 10×10^6 pfu/ml, compared with 0.3×10^6 to 3×10^6 pfu/ml).

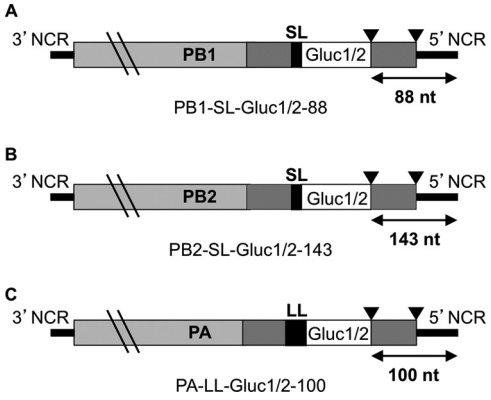

FIG. 1. **The PB1, PB2, and PA viral RNA (vRNA) segments used in reverse genetics experiments.** The vRNAs encoding PB1-Gluc1/2 (*A*), PB2-Gluc1/2 (*B*), or PA-Gluc1/2 (*C*) fusion proteins are represented schematically. The PB1-, PB2-, and PA open reading frames (light grey boxes) are fused to the sequences encoding the Gluc1 or Gluc2 (Gluc1/2) domain of *Gaussia princeps* luciferase (white boxes) and flanked by the 3′ and 5′ viral non-coding regions (NCR) (thick lines). The Gluc1 and Gluc2 domains are separated from the viral proteins with a small (PB1 and PB2) or large (PA) linker (SL and LL, respectively; black boxes). The duplicated PB1, PB2, and PA coding sequences are represented by dark grey boxes. The length of the sequence kept identical to the wild-type at the 5′ extremity of the genomic segment is indicated by a double-headed arrow. Black arrowheads indicate stop codons.

We checked whether the viral fusion proteins were indeed expressed in vP-Gluc1 and vP-Gluc2 infected cells, and whether they could participate in the reconstitution of a functional *Gaussia princeps* luciferase. To this end, MDCK cells were infected with six distinct pairs corresponding to every possible combination of vP-Gluc1 and vP-Gluc2 viruses. High luciferase activities were detected in cell lysates at 24 h post-infection (Fig. 2*A*, black bars), which likely resulted from the natural assembly of viral polymerase heterotrimers. A strong and dose-dependent reduction of luciferase activities was observed in the presence of ribavirin (Fig. 2*A*, white bars, and Fig. 2*B*) and in the presence of nucleozin (Fig. 2*C*), but not in the presence of amantadine (Fig. 2*A*, grey bars), consistent with the A/WSN/33 virus used in these experiments being sensitive to ribavirin and nucleozin but resistant to amantadine (28, 29). The observed EC_{50} values for ribavirin and nucleozin were 9.7 μM and 0.13 μM, respectively, in accordance with literature data (30, 31). These data showed that the vP-Gluc recombinant viruses were well designed for the detection of PPIs involving the polymerase subunits during the course of infection. In addition, they indicated that the vP-Gluc viruses can be used to measure the inhibition of viral

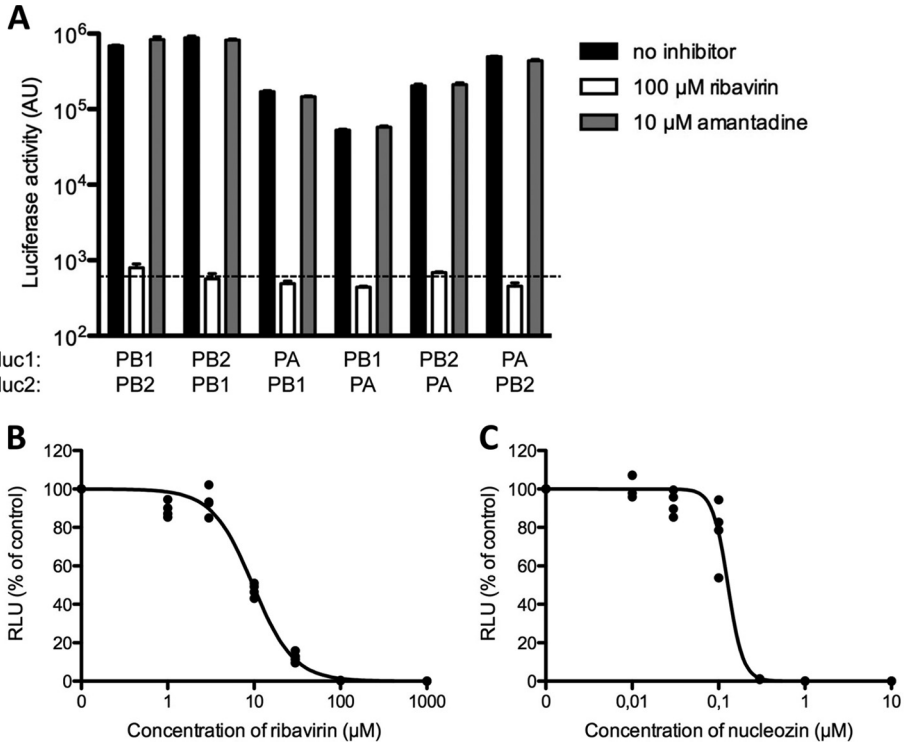

FIG. 2. **Antiviral activity assay.** *A*, luciferase activities measured in MDCK cells co-infected with six distinct indicated combinations of a vP-Gluc1 and a vP′-Gluc2 virus in the absence of antiviral compound (black bars), in the presence of 100 μM ribavirin (white bars), or in the presence of 10 μM amantadine (grey bars). Data are expressed as the mean ± Standard Deviation (S.D.) of quadruplicate repeats. Dotted line: background corresponding to the sum of the luciferase activities obtained with the P-Gluc1 or the P′-Gluc2 viruses alone. *B, C,* percentage of the luciferase activities measured in MDCK cells co-infected with the PB2-Gluc1 and PB1-Gluc2 viruses in the presence of increasing concentrations of ribavirin (*B*) or nucleozin (*C*). The data are expressed as the mean ± S.D. of quadruplicate repeats.

replication in an assay that covers the entire viral cycle, unlike existing reporter-based methods (3, 32, 33), and therefore could be instrumental for the development of improved high-throughput screens for chemical antivirals or genome-wide siRNAs.

We next explored the potential of the vP-Gluc1 viruses for the detection of binary interactions between each subunit of influenza virus polymerase (PB1, PB2, and PA) and cellular factors. To validate the assay and to determine the cutoff for non-interacting protein pairs, we selected (i) a literature-curated set (LCS) composed of 58 human proteins that were shown to interact with influenza virus polymerase through yeast two-hybrid (34 proteins) (9, 12), tandem affinity purification MS (13–15) (15 proteins), or other methods (9 proteins) (LC-Y2H, LC-MS and LC-OM in Table I and supplemental Table S1); and (ii) an *a priori* "negative" set of 36 randomly picked human proteins, or an RRS (Table I).

To identify novel host interactors of the viral polymerase subunits, we selected a set of proteins that had not been documented with respect to their interaction with influenza virus polymerase, specifically, 31 proteins annotated to the GO terms "nucleocytoplasmic transport" (GO:0006913) or "nuclear pore" (GO:0005643) (Table I and supplemental Table S1), plus 5 proteins that affected influenza virus replication in at least two independent RNAi screens (3) and were functionally related to intracellular transport (RNAi, Table I and supplemental Table S1). While this work was in progress, 10 proteins from this selection were identified as polymerase interactors (12, 13, 34) and were thus shifted into the LCS. The resulting exploratory set comprised 26 proteins (GO terms: 22 proteins; RNAi: 4 proteins) (Exp-GT and Exp-RNAi in Table I).

Expression plasmids encoding the selected human proteins fused to the Gluc2 fragment at their N-terminal end were produced. The LCS, the RRS, and the exploratory set were tested in triplicate for the production of luciferase activity upon transfection in 293T cells and subsequent infection with the recombinant influenza viruses expressing PB1-Gluc1, PB2-Gluc1, or PA-Gluc1 (Fig. 3*A*). For each human–viral protein pair, luciferase activity was expressed as an NLR over control protein pairs (18) (Fig. 3*A*).

The NLRs obtained for the RRS set are shown in Table I. The theoretical root mean square deviation with a 97.5% confidence interval obtained from Gaussian fits corresponded to NLRs of 3.2, 2.2, and 2.6 for the PB2, PB1, and PA-Gluc1 viruses, respectively (Fig. 3*B*). The NLR cutoff for non-interacting protein pairs was set accordingly at 4.0, a stringent value reducing false positive background below 2.5%.

Comparison of the results obtained in two independent experiments with the LCS and the exploratory set showed strong reproducibility (Bartlett's test for equal variances; $\chi^2(1) = 31.5642$, 25.9196, and 39.6757 for PB2-Gluc1, PB1-Gluc1, and PA-Gluc1 screens, respectively; Prob $> \chi^2 <$ 0.001; the mean NLRs are shown in Table I).

Within the LCS, 33 out of 58 proteins produced an NLR ≥4.0 with at least one of the vP-Gluc1 viruses (Table I, and Fig. 3*C*), for a recovery rate of 56.9%. The high recovery rate among proteins identified by MS (80%, 12 out of 15 proteins) or by other methods (77.8%, 7 out of 9 proteins) (Fig. 4*B*)

TABLE I
Normalized luminescence ratios (NLRs)

Gene symbol	Set[a]	NLR[b] PB2	NLR[b] PB1	NLR[b] PA
BANP	LC-Y2H	3.14	0.91	1.73
BLZF1	LC-Y2H	2.45	1.14	2.43
C10orf96	LC-Y2H	2.92	0.80	1.09
C14orf166	LC-Y2H	1.46	1.22	1.44
C1orf94	LC-Y2H	2.00	0.96	1.55
CALCOCO1	LC-Y2H	4.22	1.37	1.93
CEP70	LC-Y2H	3.18	1.41	1.68
CMTM5	LC-Y2H	2.39	1.19	2.39
COPB2	LC-MS	7.53	3.34	4.53
CRYAB	LC-Y2H	1.92	0.67	1.35
DDX3X	LC-MS	23.75	11.84	18.08
DDX5	LC-MS	31.36	13.22	17.02
DOCK8	LC-Y2H	4.80	3.32	2.90
DVL2	LC-Y2H	4.90	1.24	1.70
DVL3	LC-Y2H	5.40	2.06	2.74
eIF4E	LC-OM	14.07	9.08	11.56
FXR2	LC-Y2H	5.83	1.32	2.07
GABPB1	LC-Y2H	1.61	0.40	0.69
hnRNPM	LC-MS	26.68	10.75	14.73
HOOK1	LC-Y2H	7.93	3.46	6.33
HSP90AA1	LC-OM	3.40	1.76	3.79
IPO5	LC-MS	3.25	5.43	9.18
KCNRG	LC-Y2H	3.07	1.56	2.53
KPNA1	LC-OM	35.28	40.34	35.09
KPNA2	LC-OM	17.39	9.59	14.59
KPNA3	LC-MS	156.04	54.96	49.61
KPNA6	LC-OM	51.84	36.53	51.01
LBR	LC-MS	5.79	2.11	3.10
LNX2	LC-Y2H	1.11	0.53	0.90
MAGEA11	LC-Y2H	66.46	2.81	4.63
MAGEA6	LC-Y2H	13.48	3.03	5.70
MVP	LC-Y2H	0.64	0.41	0.63
MYO1C	LC-MS	3.64	1.81	2.72
NPM1	LC-MS	4.96	1.98	3.51
NRF1	LC-Y2H	7.71	2.02	3.48
NUP50	LC-OM	92.25	30.53	36.85
NUP54	LC-Y2H	1.46	0.84	1.40
NUP93	LC-MS	1.75	0.92	1.47
PABPC1	LC-MS	21.27	18.08	18.88
PNMA1	LC-Y2H	22.37	1.85	2.36
POLR2A	LC-OM	7.68	4.51	6.71
PTGES3	LC-MS	282.81	80.33	118.53
RAB11A	LC-OM	11.18	11.40	13.52
RABGEF1	LC-Y2H	2.20	0.79	1.36
RAN	LC-MS	7.65	8.07	5.64
RBPMS	LC-Y2H	4.37	2.53	3.69
RUVBL2	LC-MS	4.69	2.57	3.14
SIAH1	LC-Y2H	1.12	0.68	0.75
TACC1	LC-Y2H	6.94	2.22	5.24
TCF12	LC-Y2H	3.19	0.82	1.83
TFCP2	LC-Y2H	3.94	1.26	2.06
TRAF1	LC-Y2H	4.19	2.86	3.75
TRAF2	LC-Y2H	0.75	0.17	0.25
TRIP6	LC-Y2H	2.53	0.99	1.22
UBE2I	LC-Y2H	1.80	1.15	1.66
USHBP1	LC-Y2H	4.77	0.97	1.44
VISA	LC-OM	0.13	0.03	0.07
XPO7	LC-MS	3.30	1.80	2.89
AAAS	Exp-GT	2.97	1.76	2.06
AGFG1	Exp-GT	2.04	1.30	1.52
CALCOCO2	Exp-RNAi	2.06	0.59	0.80
CLIC4	Exp-RNAi	1.52	1.55	2.35
DDX19A	Exp-GT	6.24	4.65	6.92
DDX19B	Exp-GT	5.50	5.12	8.04
GLE1	Exp-GT	0.74	0.53	0.87
IPO4	Exp-GT	3.07	1.20	1.91
KPNA5	Exp-GT	34.05	27.06	26.40
NCKIPSD	Exp-GT	1.61	1.01	1.10
NUP155	Exp-GT	1.64	0.83	0.92
NUP160	Exp-GT	2.48	1.47	1.80
NUP35	Exp-GT	2.71	1.29	1.82
NUP62	Exp-GT	6.60	1.26	1.66
NUP62CL	Exp-GT	5.03	1.72	2.24
NUPL1	Exp-GT	3.40	1.89	2.20
NUPL2	Exp-GT	0.42	0.26	0.27
NUTF2	Exp-GT	1.33	0.91	1.29
NXF1	Exp-RNAi	12.03	8.96	9.74
NXT1	Exp-GT	1.50	0.88	1.20
POM121	Exp-GT	0.37	0.26	0.31
RACGAP1	Exp-RNAi	1.40	0.93	1.20
RANGAP1	Exp-GT	4.07	2.13	3.13
RBM15B	Exp-GT	11.14	7.92	10.86
SENP2	Exp-GT	3.82	2.01	2.50
SNUPN	Exp-GT	1.96	1.53	1.86
ACSL4	RRS	0.09	0.09	0.08
ADAM21	RRS	0.42	0.34	0.36
AMIGO3	RRS	0.23	0.17	0.17
APOOL	RRS	0.42	0.35	0.34
CACNG7	RRS	0.49	0.26	0.38
CD274	RRS	0.27	0.19	0.20
CNTN2	RRS	0.85	0.52	0.61
DBH	RRS	0.85	0.40	0.44
DPYSL2	RRS	1.12	0.51	0.72
FBXO40	RRS	0.96	0.89	1.23
FFAR1	RRS	0.26	0.18	0.20
GABRB2	RRS	0.29	0.22	0.19
GSTA2	RRS	2.05	1.49	1.71
GSTT1	RRS	1.02	0.52	0.78
GYPA	RRS	0.46	0.36	0.51
LRRC28	RRS	1.32	0.99	1.19
MDP1	RRS	0.92	0.56	0.53
MMP12	RRS	1.29	0.81	0.65
NCRNA00246B	RRS	1.75	0.77	1.25
NFE2L1	RRS	0.53	0.16	0.29
NHEDC1	RRS	1.08	0.85	0.88
NXPH1	RRS	0.76	0.60	0.64
OR2B6	RRS	0.44	0.32	0.33
PLEKHA9	RRS	0.60	0.53	0.64
PLVAP	RRS	0.58	0.34	0.53
PTPRE	RRS	0.17	0.15	0.18
RHBDD2	RRS	0.28	0.18	0.27
SAA2	RRS	0.36	0.26	0.32
SEMA3C	RRS	1.31	0.98	0.87
SLC7A13	RRS	0.81	0.41	0.41
SPINK1	RRS	0.66	0.59	0.74
TOP3B	RRS	3.36	3.21	2.98
TRPT1	RRS	2.45	2.20	2.75
UGT3A1	RRS	1.31	1.06	1.12
XKR6	RRS	0.28	0.25	0.22
ZNF131	RRS	1.64	1.38	1.67

[a] LC, literature-curated; Y2H, yeast two-hybrid; MS, mass spectrometry; OM, other methods; Exp, experimental; GT, GO terms; RRS, random reference set.

[b] Mean from two independent determinations.

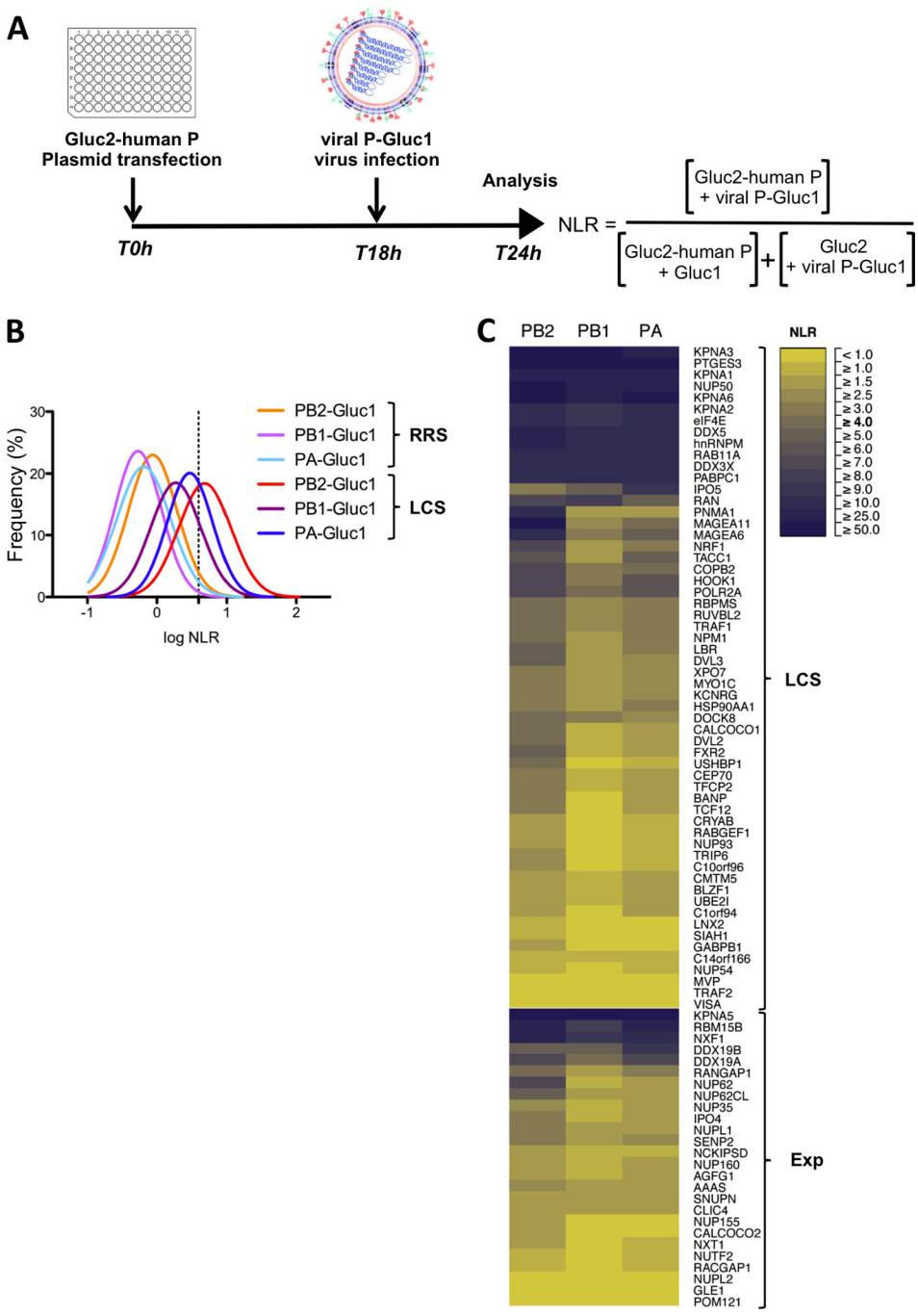

FIG. 3. **Identification of cellular interactors of influenza virus polymerase via iPCA.** *A*, schematic of the experiment. 293T cells seeded in 96-well plates were transfected with an ordered set of 84 plasmids encoding human proteins fused to Gluc2 (Gluc2-human P), or with control plasmids. At 18 h post-transfection, 293T cells were infected at a high multiplicity of infection (>1 pfu/cell) with an influenza virus expressing a Gluc1-tagged polymerase (viral P-Gluc1) or with the wild-type control virus. At 6 h post-infection, cell lysates were prepared and normalized luminescence ratios (NLRs) were determined by dividing the luminescence activity measured in cells co-expressing a Gluc2-human P and a viral P-Gluc1 by the sum of the luminescence activities measured in the corresponding control samples. *B*, Gaussian curves fitted on log(NLR) values of the random reference set (RRS) and the literature-curated set (LCS) with the PB2-Gluc1, PB1-Gluc1, and PA-Gluc1 viruses. The positive threshold value of 4 is indicated. *C*, heat map of the NLRs. The 84 screened cellular proteins are arranged by hierarchical clustering according to their NLRs. The 58 proteins that belong to the LCS and the 26 proteins that belong to the exploratory set (Exp) are indicated. The color scale indicates the range of NLRs measured upon screening with PB2-Gluc1, PB1-Gluc1, or PA-Gluc1 recombinant influenza virus.

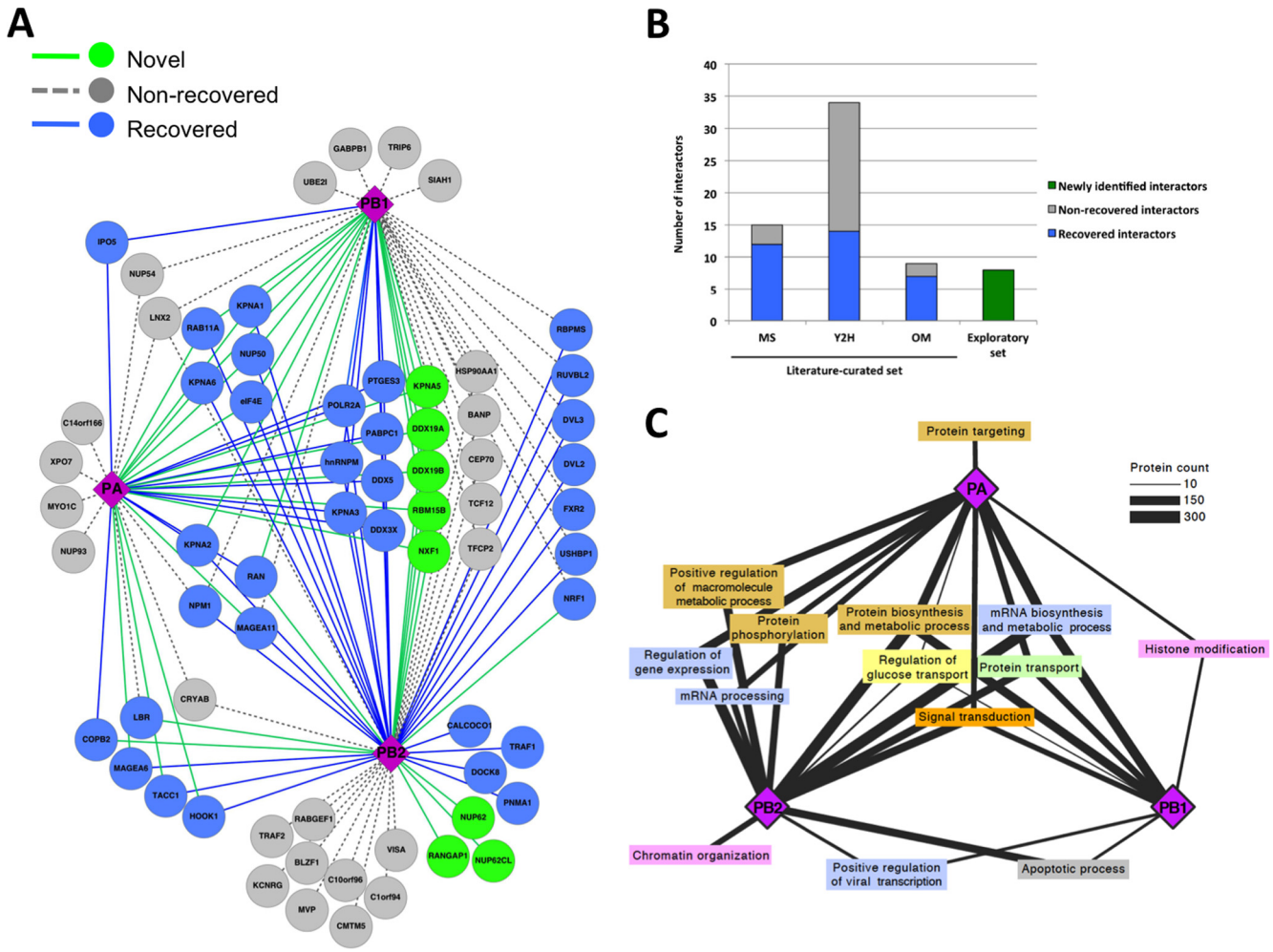

FIG. 4. **Analysis of cellular interactors of influenza virus polymerase.** *A*, influenza virus polymerase interaction network. Viral polymerase subunits are represented by pink diamonds. Cellular interactors are represented by circles colored according to the recovery (blue), non-recovery (gray), or novelty (green) of the interaction. *B*, histogram representation of the number of recovered/non-recovered interactors among the mass-spectrometry (MS), yeast two-hybrid (Y2H), and other-method (OM) reference subsets within the literature-curated set, and the number of newly identified interactors among the exploratory set. *C*, ClueGO visualization as a functionally grouped annotation network with lines connecting polymerase subunits to gene ontology biological process attributes. Line width is proportional to the relative enrichment of the biological processes evaluated by protein count.

underlines the sensitivity of our assay. The lower recovery rate among proteins identified by means of yeast two-hybrid screening is in agreement with the fact that some biophysical interactions that can be forced in the context of yeast two-hybrid cannot be recovered in the context of human cell expression, and thus correspond to biological false positives (35). The proportion of false negatives might be further reduced by reversing Gluc1 and Gluc2 fusion with respect to viral and host proteins, which might modulate the background signal, and by testing both N- and C-terminal fusions with host proteins, as N-terminal fusions may disrupt protein–protein interactions in some cases. Moreover, new edges were identified within the LCS; that is, some of the proteins that had been shown to interact with one of the viral polymerase subunits in pair-wise screens were found to interact with another subunit as well (Fig. 4*A*, green edges connected to blue nodes), most likely indicating an interaction with a heterodimer or with the PB1-PB2-PA heterotrimer. Supporting the accuracy of this interpretation is the fact that the importin 5 protein, known to interact with the PB1-PA dimer but not with the PB2 protein (36), produced NLRs ≥4.0 with the PB1- and PA-Gluc1 viruses but not with the PB2-Gluc1 virus (Table I and Fig. 4*A*).

Within the exploratory set, 8 out of 26 proteins produced an NLR > 4.0 with at least one of the vP-Gluc1 viruses (Table I and Fig. 3*C*) and were thus identified as novel interactors of the viral polymerase (Fig. 4*A*, green nodes). These include the DDX19A and DDX19B helicases, the karyopherin alpha 5 (KPNA5), the NUP62 nucleoporin, and NUP62CL, a shorter protein that shows 79% similarity with the C-terminal domain of NUP62, Ran GTPase activating protein 1 (RANGAP1), putative RNA binding motif protein 15B (RBM15B), and nuclear

RNA export factor 1 (NXF1). The NUP62, NUP62CL, and RANGAP1 proteins interacted with PB2 only, whereas the five other proteins interacted with all three polymerase subunits (Fig. 4*A*). Karyopherin alpha 5 and Ran GTPase activating protein 1, a regulator of the Ran GTP/GDP cycle, are involved in the nuclear import pathway. NUP62 and DDX19B are components of the nuclear pore complex and, along with NXF1 and its cofactor RBM15B, are involved in mRNA export from the nucleus.

In order to extract functional information from our interactomic dataset, we started by selecting the 41 host proteins that were found to interact with influenza virus polymerase subunits in infectious native conditions using the iPCA assay (Fig. 4*A*, blue and green nodes). Based on this selection, identified herein as "layer one," we generated a second layer of human proteins corresponding to their first neighbors in the HIPPIE high-confidence score filtered network for human PPIs (24) (see "Experimental Procedures" for scoring). To capture biological information associated with the subnetwork of the human interactome resulting from the merging of both interactomic layers, we used ClueGO, a Cytoscape plugin that extracts and statistically analyzes GO annotations (25) (see "Experimental Procedures" for details on the enrichment analysis). The functionally grouped annotation network obtained with ClueGO (Fig. 4*C*) showed enrichment for processes related to mRNA and protein biosynthesis and metabolism, protein transport, and apoptosis, in agreement with the fact that these processes can be hijacked or modulated by influenza virus infection (3). In addition, this functional enrichment analysis suggested the interaction of the polymerase subunits with the chromatin compartment and with signal transduction pathways, in agreement with recent studies (9, 37–39). Interestingly, some of the enriched processes were connected with only two or one of the viral polymerase subunits (Fig. 4*C*), highlighting their specificities.

We performed siRNA-mediated knockdown on two novel interactors of the viral polymerase identified via iPCA, RANGAP1 and NUP62, in order to investigate their role in influenza virus replication. A549 cells treated with siRNAs targeting RANGAP1 or NUP62 or with a non-targeting control siRNA were infected with the A/WSN/33 influenza virus at an MOI of 0.001 or with VSV at an MOI of 0.0001. CCT2 siRNA was used as a positive control, as it has been shown to reduce influenza virus growth in A549 cells (40). At 24 h post-infection, supernatants were harvested and virus titers were determined via plaque assays (Fig. 5). siRNA-mediated knockdown of CCT2, RANGAP1, and NUP62 reduced the expression of target mRNAs by more than 80% as evaluated by RT-qPCR and showed no toxicity (data not shown). Down-regulation of CCT2 and RANGAP1 expression inhibited influenza virus replication by 3.4- and 4.5-fold, respectively. In NUP62-silenced cells, a 22.3-fold reduction in influenza virus titers was observed (Fig. 5). In contrast, CCT2, RANGAP1, and NUP62 siRNAs did not affect VSV replication (data not shown). These data clearly demonstrate that NUP62 and RANGAP1 are involved in influenza virus replication.

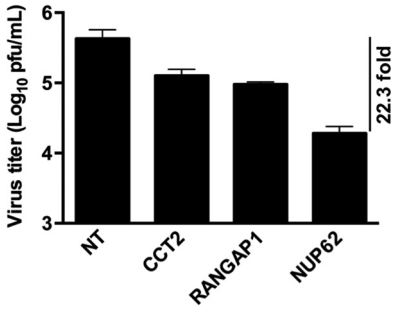

FIG. 5. **Influenza virus replication in siRNA-treated A549 cells.** A549 cells were transfected with siRNA targeting CCT2, RANGAP1, or NUP62 or with non-target siRNA (NT). At 48 h post-transfection, cells were infected with influenza A/WSN/33 virus at an MOI of 0.001. Supernatants from infected cells were harvested at 24 h post-infection, and viral titers were determined via plaque assay on MDCK cells. The data are expressed as the mean ± S.D. of independent triplicate repeats.

DISCUSSION

Transcription and replication of the genome of influenza A virus take place in the nuclei of the infected cells. In order to gain access to the nucleus, the viral RNPs and the newly synthetized polymerase subunits must interact with the host nuclear import machinery (11, 41). Import of macromolecules through the nuclear pore complex (NPC) is mediated by import receptors such as importins or karyopherins that bind the cargo, interact with nucleoporins, and facilitate translocation through the NPC (42). Within the LCS, we confirmed the interaction of one or several viral polymerase subunits with importins IPO5 (importin 5, previously known as RANBP5), KPNA1 (importin alpha 5), KPNA2 (importin alpha 1), KPNA3 (importin alpha 4), and KPNA6 (importin alpha 7) and with the nucleoporin NUP50, which has been proposed to prevent nuclear PB2 from rebinding to importin alpha 5 (11, 34, 41). Within the exploratory set, we identified KPNA5 (importin alpha 6), RANGAP1, NUP62, and NUP62CL as additional partners. KPNA5 shares more than 90% similarity with KPNA1 and KPNA6, and human KPNA5 expression seems to be restricted to the testis (43). KPNA5 might be a species-specific importin, as mouse KPNA5 has not been identified, whereas bovine KPNA5 was found to be expressed ubiquitously (44). The relative importance of KPNA5 and its potential redundancy with KPNA1 and KPNA6 are thus likely to differ from species to species, in line with the fact that the differential use of importin alpha isoforms by influenza virus is a determinant of host range (11, 45). Inside the nucleus, the small GTPase Ran in a GTP-bound form binds to importins and enables their dissociation from the cargo and their translocation to the cytoplasm. The cytoplasmic Ran GTPase activating protein RANGAP1 stimulates the GTPase activity of Ran, which results in the release of importins for another

import cycle (42). An interaction between the viral polymerase and RANGAP1 could thus modulate the recycling of importins or other transport receptors. NUP62 is a nucleoporin located at the core of the NPC, and NUP62CL is a shorter protein that shows 79% similarity with the C-terminal domain of NUP62. Our findings add influenza virus polymerase to the list of other viral proteins known to interact with NUP62, such as HTLV Tax, HSV ICP27, or EBV BGLF4 proteins (46–48). Several viruses interfere with nucleocytoplasmic transport via the degradation or disruption (or both) of nucleoporins. In particular, NUP62 is cleaved by enterovirus protease 2A, hyperphosphorylated by cardiovirus L protein, and displaced from the NPC upon adenovirus or HIV-1 infection (49). Our gene silencing experiments demonstrate that NUP62 is required for efficient influenza virus replication. It remains to be explored how NUP62 is involved in viral replication, whether the interaction between influenza virus polymerase and NUP62 enhances the transport of viral RNPs or viral mRNAs across the NPC, and whether it could alter the nucleocytoplasmic trafficking of host factors or mRNAs.

NXF1, the major cellular transport receptor for the export of cellular mRNAs, was identified in four independent RNAi screens as an important host factor for influenza virus replication (3, 5–7, 9). Indeed, a subset of influenza virus mRNAs is exported through the NXF1 pathway (50). However, the mechanisms by which influenza virus mRNAs are exported to the cytoplasm are unclear. The question of whether the viral polymerase is associated with any or a subset of viral mRNAs remains controversial (51–53). Here we have clearly demonstrated an association of influenza virus polymerase with NXF1 and with the NXF1-cofactor RMB15B (54). Moreover, we have shown that influenza virus polymerase interacts with DDX19B (and DDX19A, which shows 98% similarity with DDX19B), a DEAD-box helicase that localizes to the cytoplasmic side of the NPC by binding to NUP214 and which plays an essential role in mRNA export by remodeling mRNP complexes during their passage through the NPC (55). The interaction of the viral polymerase with these mRNA export factors is likely to modulate the export of cellular and/or viral mRNAs. Taken together, our findings should contribute to a better understanding of the molecular mechanisms by which influenza viruses exploit the host nucleocytoplasmic trafficking pathways for their replication.

We report the first application of luciferase complementation to proteins expressed in the context of an infectious pathogen. Our iPCA assay allows the detection of binary protein–protein interactions in infectious, native conditions. We illustrate how this assay can be combined with an annotated human protein–protein interaction network to generate a high-confidence function-specific subnetwork used by the influenza virus. The fact that it covers the pathogen's entire life cycle represents a clear advantage over the yeast two-hybrid screen. This feature is also very useful for the development of high-throughput screens for chemical antivirals or genome-wide siRNAs. The iPCA assay can readily be handled inside high-security laboratories. As a consequence, it applies to highly pathogenic microorganisms, unlike mass spectrometry, which does not apply to infectious cell lysates that cannot be handled experimentally outside high-security laboratories. It showed excellent sensitivity and accuracy when applied to influenza virus against random, literature-curated, and exploratory sets of human proteins, as were able to confirm most of the already documented influenza polymerase–host interactions and to identify novel interactions. These observations suggest that fusion to the small-sized GLuc1 or GLuc2 fragment is overall well tolerated and preserves protein–protein interactions. The iPCA assay or adaptations of it should prove useful in elucidating many aspects of influenza virus biology. With more infectious reverse genetics systems becoming available, this strategy should be widely applicable to other viral and non-viral pathogens.

Acknowledgments—We are grateful to George Brownlee for providing the plasmids for reverse genetics of the A/WSN/33 strain, to Yasmina Fortier and Dorothée Moisy for assistance with some experiments, and to Marie-Anne Rameix-Welti and Xingyi Ge for useful discussions. We thank Michael Cusick for a critical reading of the manuscript.

* This work was funded by the Institut Pasteur (DARRI Project 2010-790294) and by the European Commission funded FP7 projects FLUPHARM (Grant Agreement No. 259751) and PREDEMICS (Grant Agreement No. 278433). Thomas Rolland was supported by Grant Nos. U01-HG001715 and R01-HG006061 from the National Human Genome Research Institute.

S This article contains supplemental material.

‡‡ To whom correspondence should be addressed: E-mail: nadia.naffakh@pasteur.fr or yves_jacob@DFCI.HARVARD.edu.

REFERENCES

1. Shaw, M. L. (2011) The host interactome of influenza virus presents new potential targets for antiviral drugs. *Rev. Med. Virol.* **21,** 358–369
2. Lee, S. M., and Yen, H. L. (2012) Targeting the host or the virus: current and novel concepts for antiviral approaches against influenza virus infection. *Antiviral Res.* **96,** 391–404
3. Watanabe, T., Watanabe, S., and Kawaoka, Y. (2010) Cellular networks involved in the influenza virus life cycle. *Cell Host Microbe* **7,** 427–439
4. Stertz, S., and Shaw, M. L. (2011) Uncovering the global host cell requirements for influenza virus replication via RNAi screening. *Microbes Infect.* **13,** 516–525
5. Brass, A. L., Huang, I. C., Benita, Y., John, S. P., Krishnan, M. N., Feeley, E. M., Ryan, B. J., Weyer, J. L., van der Weyden, L., Fikrig, E., Adams, D. J., Xavier, R. J., Farzan, M., and Elledge, S. J. (2009) The IFITM proteins mediate cellular resistance to influenza A H1N1 virus, West Nile virus, and dengue virus. *Cell* **139,** 1243–1254
6. Hao, L., Sakurai, A., Watanabe, T., Sorensen, E., Nidom, C. A., Newton, M. A., Ahlquist, P., and Kawaoka, Y. (2008) Drosophila RNAi screen identifies host genes important for influenza virus replication. *Nature* **454,** 890–893
7. Karlas, A., Machuy, N., Shin, Y., Pleissner, K. P., Artarini, A., Heuer, D., Becker, D., Khalil, H., Ogilvie, L. A., Hess, S., Mäurer, A. P., Müller, E., Wolff, T., Rudel, T., and Meyer, T. F. (2010) Genome-wide RNAi screen identifies human host factors crucial for influenza virus replication. *Nature* **463,** 818–822
8. König, R., Stertz, S., Zhou, Y., Inoue, A., Hoffmann, H. H., Bhattacharyya, S., Alamares, J. G., Tscherne, D. M., Ortigoza, M. B., Liang, Y., Gao, Q., Andrews, S. E., Bandyopadhyay, S., De Jesus, P., Tu, B. P., Pache, L., Shih, C., Orth, A., Bonamy, G., Miraglia, L., Ideker, T., García-Sastre, A.,

Young, J. A., Palese, P., Shaw, M. L., and Chanda, S. K. (2010) Human host factors required for influenza virus replication. *Nature* **463,** 813–817
9. Shapira, S. D., Gat-Viks, I., Shum, B. O., Dricot, A., de Grace, M. M., Wu, L., Gupta, P. B., Hao, T., Silver, S. J., Root, D. E., Hill, D. E., Regev, A., and Hacohen, N. (2009) A physical and regulatory map of host-influenza interactions reveals pathways in H1N1 infection. *Cell* **139,** 1255–1267
10. Naffakh, N., Tomoiu, A., Rameix-Welti, M. A., and van der Werf, S. (2008) Host restriction of avian influenza viruses at the level of the ribonucleoproteins. *Annu. Rev. Microbiol.* **62,** 403–424
11. Resa-Infante, P., and Gabriel, G. (2013) The nuclear import machinery is a determinant of influenza virus host adaptation. *Bioessays* **35,** 23–27
12. Tafforeau, L., Chantier, T., Pradezynski, F., Pellet, J., Mangeot, P. E., Vidalain, P. O., Andre, P., Rabourdin-Combe, C., and Lotteau, V. (2011) Generation and comprehensive analysis of an influenza virus polymerase cellular interaction network. *J. Virol.* **85,** 13010–13018
13. Bradel-Tretheway, B. G., Mattiacio, J. L., Krasnoselsky, A., Stevenson, C., Purdy, D., Dewhurst, S., and Katze, M. G. (2011) Comprehensive proteomic analysis of influenza virus polymerase complex reveals a novel association with mitochondrial proteins and RNA polymerase accessory factors. *J. Virol.* **85,** 8569–8581
14. Jorba, N., Juarez, S., Torreira, E., Gastaminza, P., Zamarreño, N., Albar, J. P., and Ortín, J. (2008) Analysis of the interaction of influenza virus polymerase complex with human cell factors. *Proteomics* **8,** 2077–2088
15. Mayer, D., Molawi, K., Martínez-Sobrido, L., Ghanem, A., Thomas, S., Baginsky, S., Grossmann, J., García-Sastre, A., and Schwemmle, M. (2007) Identification of cellular interaction partners of the influenza virus ribonucleoprotein complex and polymerase complex using proteomic-based approaches. *J. Proteome Res.* **6,** 672–682
16. De Las Rivas, J., and Fontanillo, C. (2010) Protein-protein interactions essentials: key concepts to building and analyzing interactome networks. *PLoS Comput. Biol.* **6,** e1000807
17. Resa-Infante, P., Jorba, N., Coloma, R., and Ortin, J. (2011) The influenza virus RNA synthesis machine: advances in its structure and function. *RNA Biol.* **8,** 207–215
18. Cassonnet, P., Rolloy, C., Neveu, G., Vidalain, P. O., Chantier, T., Pellet, J., Jones, L., Muller, M., Demeret, C., Gaud, G., Vuillier, F., Lotteau, V., Tangy, F., Favre, M., and Jacob, Y. (2011) Benchmarking a luciferase complementation assay for detecting protein complexes. *Nat. Methods* **8,** 990–992
19. Remy, I., and Michnick, S. W. (2006) A highly sensitive protein-protein interaction assay based on Gaussia luciferase. *Nat. Methods* **3,** 977–979
20. Fodor, E., Devenish, L., Engelhardt, O. G., Palese, P., Brownlee, G. G., and García-Sastre, A. (1999) Rescue of influenza A virus from recombinant DNA. *J. Virol.* **73,** 9679–9682
21. Matrosovich, M., Matrosovich, T., Garten, W., and Klenk, H. D. (2006) New low-viscosity overlay medium for viral plaque assays. *Virol. J.* **3,** 63
22. Avilov, S. V., Moisy, D., Munier, S., Schraidt, O., Naffakh, N., and Cusack, S. (2012) Replication-competent influenza A virus that encodes a split-green fluorescent protein-tagged PB2 polymerase subunit allows live-cell imaging of the virus life cycle. *J. Virol.* **86,** 1433–1448
23. Braun, P., Tasan, M., Dreze, M., Barrios-Rodiles, M., Lemmens, I., Yu, H., Sahalie, J. M., Murray, R. R., Roncari, L., de Smet, A. S., Venkatesan, K., Rual, J. F., Vandenhaute, J., Cusick, M. E., Pawson, T., Hill, D. E., Tavernier, J., Wrana, J. L., Roth, F. P., and Vidal, M. (2009) An experimentally derived confidence score for binary protein-protein interactions. *Nat. Methods* **6,** 91–97
24. Schaefer, M. H., Fontaine, J. F., Vinayagam, A., Porras, P., Wanker, E. E., and Andrade-Navarro, M. A. (2012) HIPPIE: integrating protein interaction networks with experiment based quality scores. *PLoS One* **7,** e31826
25. Bindea, G., Mlecnik, B., Hackl, H., Charoentong, P., Tosolini, M., Kirilovsky, A., Fridman, W. H., Pages, F., Trajanoski, Z., and Galon, J. (2009) ClueGO: a Cytoscape plug-in to decipher functionally grouped gene ontology and pathway annotation networks. *Bioinformatics* **25,** 1091–1093
26. Dos Santos Afonso, E., Escriou, N., Leclercq, I., van der Werf, S., and Naffakh, N. (2005) The generation of recombinant influenza A viruses expressing a PB2 fusion protein requires the conservation of a packaging signal overlapping the coding and noncoding regions at the 5′ end of the PB2 segment. *Virology* **341,** 34–46
27. Neumann, G., and Kawaoka, Y. (1999) Genetic engineering of influenza and other negative-strand RNA viruses containing segmented genomes. *Adv. Virus Res.* **53,** 265–300
28. Sidwell, R. W., Bailey, K. W., Wong, M. H., Barnard, D. L., and Smee, D. F. (2005) In vitro and in vivo influenza virus-inhibitory effects of viramidine. *Antiviral Res.* **68,** 10–17
29. Takeda, M., Pekosz, A., Shuck, K., Pinto, L. H., and Lamb, R. A. (2002) Influenza a virus M2 ion channel activity is essential for efficient replication in tissue culture. *J. Virol.* **76,** 1391–1399
30. Kao, R. Y., Yang, D., Lau, L. S., Tsui, W. H., Hu, L., Dai, J., Chan, M. P., Chan, C. M., Wang, P., Zheng, B. J., Sun, J., Huang, J. D., Madar, J., Chen, G., Chen, H., Guan, Y., and Yuen, K. Y. (2010) Identification of influenza A nucleoprotein as an antiviral target. *Nat. Biotechnol.* **28,** 600–605
31. Smee, D. F., Morrison, A. C., Barnard, D. L., and Sidwell, R. W. (2002) Comparison of colorimetric, fluorometric, and visual methods for determining anti-influenza (H1N1 and H3N2) virus activities and toxicities of compounds. *J. Virol. Methods* **106,** 71–79
32. Martínez-Sobrido, L., Cadagan, R., Steel, J., Basler, C. F., Palese, P., Moran, T. M., and García-Sastre, A. (2010) Hemagglutinin-pseudotyped green fluorescent protein-expressing influenza viruses for the detection of influenza virus neutralizing antibodies. *J. Virol.* **84,** 2157–2163
33. Wang, W., Butler, E. N., Veguilla, V., Vassell, R., Thomas, J. T., Moos, M., Ye, Z., Hancock, K., and Weiss, C. D. (2008) Establishment of retroviral pseudotypes with influenza hemagglutinins from H1, H3, and H5 subtypes for sensitive and specific detection of neutralizing antibodies. *J. Virol. Methods* **153,** 111–119
34. Pumroy, R. A., Nardozzi, J. D., Hart, D. J., Root, M. J., and Cingolani, G. (2012) Nucleoporin Nup50 stabilizes closed conformation of armadillo repeat 10 in importin α5. *J. Biol. Chem.* **287,** 2022–2031
35. Dreze, M., Monachello, D., Lurin, C., Cusick, M. E., Hill, D. E., Vidal, M., and Braun, P. (2010) High-quality binary interactome mapping. *Methods Enzymol.* **470,** 281–315
36. Deng, T., Engelhardt, O. G., Thomas, B., Akoulitchev, A. V., Brownlee, G. G., and Fodor, E. (2006) Role of ran binding protein 5 in nuclear import and assembly of the influenza virus RNA polymerase complex. *J. Virol.* **80,** 11911–11919
37. Alfonso, R., Lutz, T., Rodriguez, A., Chavez, J. P., Rodriguez, P., Gutierrez, S., and Nieto, A. (2011) CHD6 chromatin remodeler is a negative modulator of influenza virus replication that relocates to inactive chromatin upon infection. *Cell Microbiol.* **13,** 1894–1906
38. Chase, G. P., Rameix-Welti, M. A., Zvirbliene, A., Zvirblis, G., Gotz, V., Wolff, T., Naffakh, N., and Schwemmle, M. (2011) Influenza virus ribonucleoprotein complexes gain preferential access to cellular export machinery through chromatin targeting. *PLoS Pathog.* **7,** e1002187
39. Graef, K. M., Vreede, F. T., Lau, Y. F., McCall, A. W., Carr, S. M., Subbarao, K., and Fodor, E. (2010) The PB2 subunit of the influenza virus RNA polymerase affects virulence by interacting with the mitochondrial antiviral signaling protein and inhibiting expression of beta interferon. *J. Virol.* **84,** 8433–8445
40. Fislova, T., Thomas, B., Graef, K. M., and Fodor, E. (2010) Association of the influenza virus RNA polymerase subunit PB2 with the host chaperonin CCT. *J. Virol.* **84,** 8691–8699
41. Hutchinson, E. C., and Fodor, E. (2012) Nuclear import of the influenza A virus transcriptional machinery. *Vaccine* **30,** 7353–7358
42. Stewart, M. (2007) Molecular mechanism of the nuclear protein import cycle. *Nat. Rev. Mol. Cell Biol.* **8,** 195–208
43. Kohler, M., Ansieau, S., Prehn, S., Leutz, A., Haller, H., and Hartmann, E. (1997) Cloning of two novel human importin-alpha subunits and analysis of the expression pattern of the importin-alpha protein family. *FEBS Lett.* **417,** 104–108
44. Tejomurtula, J., Lee, K. B., Tripurani, S. K., Smith, G. W., and Yao, J. (2009) Role of importin alpha8, a new member of the importin alpha family of nuclear transport proteins, in early embryonic development in cattle. *Biol. Reprod.* **81,** 333–342
45. Gabriel, G., Klingel, K., Otte, A., Thiele, S., Hudjetz, B., Arman-Kalcek, G., Sauter, M., Shmidt, T., Rother, F., Baumgarte, S., Keiner, B., Hartmann, E., Bader, M., Brownlee, G. G., Fodor, E., and Klenk, H. D. (2011) Differential use of importin-α isoforms governs cell tropism and host adaptation of influenza virus. *Nat. Commun.* **2,** 156
46. Chang, C. W., Lee, C. P., Huang, Y. H., Yang, P. W., Wang, J. T., and Chen, M. R. (2012) Epstein-Barr virus protein kinase BGLF4 targets the nucleus through interaction with nucleoporins. *J. Virol.* **86,** 8072–8085

47. Malik, P., Tabarraei, A., Kehlenbach, R. H., Korfali, N., Iwasawa, R., Graham, S. V., and Schirmer, E. C. (2012) Herpes simplex virus ICP27 protein directly interacts with the nuclear pore complex through Nup62, inhibiting host nucleocytoplasmic transport pathways. *J. Biol. Chem.* **287,** 12277–12292
48. Tsuji, T., Sheehy, N., Gautier, V. W., Hayakawa, H., Sawa, H., and Hall, W. W. (2007) The nuclear import of the human T lymphotropic virus type I (HTLV-1) tax protein is carrier- and energy-independent. *J. Biol. Chem.* **282,** 13875–13883
49. Cohen, S., Etingov, I., and Pante, N. (2012) Effect of viral infection on the nuclear envelope and nuclear pore complex. *Int. Rev. Cell Mol. Biol.* **299,** 117–159
50. Read, E. K., and Digard, P. (2010) Individual influenza A virus mRNAs show differential dependence on cellular NXF1/TAP for their nuclear export. *J. Gen. Virol.* **91,** 1290–1301
51. Bier, K., York, A., and Fodor, E. (2011) Cellular cap-binding proteins associate with influenza virus mRNAs. *J. Gen. Virol.* **92,** 1627–1634
52. Burgui, I., Yángüez, E., Sonenberg, N., and Nieto, A. (2007) Influenza virus mRNA translation revisited: is the eIF4E cap-binding factor required for viral mRNA translation? *J. Virol.* **81,** 12427–12438
53. Shih, S. R., and Krug, R. M. (1996) Surprising function of the three influenza viral polymerase proteins: selective protection of viral mRNAs against the cap-snatching reaction catalyzed by the same polymerase proteins. *Virology* **226,** 430–435
54. Uranishi, H., Zolotukhin, A. S., Lindtner, S., Warming, S., Zhang, G. M., Bear, J., Copeland, N. G., Jenkins, N. A., Pavlakis, G. N., and Felber, B. K. (2009) The RNA-binding motif protein 15B (RBM15B/OTT3) acts as cofactor of the nuclear export receptor NXF1. *J. Biol. Chem.* **284,** 26106–26116
55. Folkmann, A. W., Noble, K. N., Cole, C. N., and Wente, S. R. (2011) Dbp5, Gle1-IP6 and Nup159: a working model for mRNP export. *Nucleus* **2,** 540–548